IET Communications

Research Article

IET Journals
The Institution of Engineering and Technology

Approach for determining the optimum pilot placement in orthogonal frequency division multiplexing systems

ISSN 1751-8628
Received on 26th September 2014
Revised on 27th April 2015
Accepted on 24th June 2015
doi: 10.1049/iet-com.2015.0104
www.ietdl.org

Begüm Korunur Engiz[1], *Çetin Kurnaz*[2] ✉, *Hatice Sezgin*[2]

[1]*Fatsa Faculty of Marine Sciences, Ordu University, Ordu, Turkey*
[2]*Department of Electrical and Electronics Engineering, Ondokuz Mayis University, Samsun, Turkey*
✉ *E-mail: ckurnaz@omu.edu.tr*

Abstract: One of the major concerns in wireless communications is multipath fading that causes some adverse effects and significantly limits the performance of a system. To overcome these effects in orthogonal frequency division multiplexing, system channel estimation must be performed. Pilot arrangement is very crucial in pilot aided channel estimation. There is an inevitable trade-off between the number of pilot symbols used in channel estimation, the accuracy of such estimation, and spectral efficiency. In this study, the analytical formulation of the channel estimation mean squared error based on a channel's sampled power density is presented. A novel mathematical rule for the optimum pilot symbol interval and a novel adaptive pilot placement are proposed to improve channel estimation quality and bandwidth efficiency. The optimum pilot symbol intervals which are related to channels' coherence times and coherence bandwidths can be calculated easily with the use of the proposed method. As the proposed method effectively reduces the number of searches for the optimum pilot symbol interval, it gives rise to simply constructing adaptive pilot placement in real-time systems. Compared with fixed pilot placement, the proposed adaptive placement shows obvious improvement up to 6% in bandwidth efficiency while maintaining the bit error rate performance.

1 Introduction

Orthogonal frequency division multiplexing (OFDM), a form of multicarrier modulation, has recently become highly appealing for wireless communication systems for major advantages such as efficient use of available spectrum, increased robustness to frequency selective fading, higher data rate transmission capability, and enhanced capability to combat intersymbol interference (ISI) and intercarrier interference (ICI).

In wireless systems, transmitted information reaches receivers after passing through a radio channel. In OFDM systems, to adapt the system to radio channel variations, to lower bit error rate (BER), and hence to increase the system performance, an appropriate channel estimation method must be applied depending on the type of fading. Channel estimation methods can be grouped into two categories: non-pilot aided and pilot aided. Due to the limitations of non-pilot aided algorithms such as the requirement of statistical knowledge of received signal, the pilot aided channel estimation is more effectual, hence have become more popular [1].

One-dimensional pilot aided channel estimation can be performed by either inserting pilot symbols into all of the subcarriers of OFDM symbols with a specific period (block type) or inserting pilot tones into each OFDM symbol (comb type), which requires an efficient interpolation technique [2]. It is shown in [2] that low-pass interpolation yields the minimum BER. Since radio channel is frequency selective and time varying, pilots can be scattered as two dimensional (2D) in both time and frequency, which allows better tracking of channels. Therefore, designing an effective 2D pilot pattern is very crucial and addressed in many works [3–5].

The channel estimation accuracy can be improved by choosing proper pilot pattern according to a channel's type of selectivity and/or increasing the pilot density. There is an inevitable trade-off between the channel estimation accuracy and the spectral efficiency of the system. Using more pilot symbols reduces the spectral efficiency while increasing the system performance and vice versa. Therefore, determining the pilot pattern that yields higher spectral efficiency, higher estimation accuracy, and lower computational complexity is very crucial.

The frequency selective channel estimation problem in OFDM is investigated from the perspective of compressed sensing (CS), two criteria for optimising the pilot pattern for CS-based channel estimation is proposed in [5], and better channel estimation mean squared error (MSE) and BER performance is obtained by the use of the optimised pilot pattern without computational complexity. In [6] a new tight bound for the number of used pilots in channel estimation for OFDM systems is driven, and system performance is improved compared with the conventional schemes by using this bound. To estimate fading channel, a new method based on wavelet decomposition is presented in [7]. By using this method, noise effect is reduced, and the system becomes more robust to changes in modulation parameters and pilot spacing; thus, better channel estimation is obtained. To optimise the placement of the pilot tones in SISO and MIMO, a transmitter algorithm is proposed in [8]. The optimiser that is based on differential evolution adapts the time frequency pilot spaces according to the changes in the channel's delay spread and Doppler spread as well as pilot power allocation, resulting in optimal pilot designs with affordable computational costs. In [9], a novel low complexity channel estimator for OFDM systems with irregular pilot arrangement is proposed and the impact of pilot arrangement on channel estimation MSE is analysed. The analytical formulation of the channel estimation MSE as a function of the pilot density for a given power efficiency is presented in [10], and it is confirmed that the optimum density is the one that closely fulfils the 2D sampling theorem via simulations and analytical results. In [11], optimal pilot symbol design for time invariant scenarios is investigated, analytical expressions for the optimal distance between adjacent pilot symbols and the optimal power distribution between pilot symbols and data symbols are obtained, and with the use of this system, approximately 30% capacity gain is achieved. In [12], the effect of pilot arrangement on OFDM system performance for different time and frequency selective fading channels is evaluated in terms of BER and the relationship

© The Institution of Engineering and Technology 2015

between the optimum pilot intervals, channels' coherence time (T_c), and coherence bandwidth (B_c) is determined.

In this study, the design of the optimal 2D rectangular pilot pattern so as to minimise the MSE of the estimated channel impulse response (CIR) is proposed. First, the optimum pilot symbols in frequency and time direction are analytically derived based on channels' sampled power spectral density. Then, a novel mathematical method is proposed that relates the optimum pilot symbol intervals to a channel's coherence bandwidth and coherence time. Based on the proposed method, a new adaptively changing pilot placement is suggested and verified by computer simulations. Compared with fixed pilot placement, with the use of the adaptive placement, higher bandwidth efficiency is achieved without performance loss.

2 OFDM system and wireless channel characteristics

In a pilot aided channel estimation based system, the input data is divided into blocks called OFDM symbols. A cyclic prefix (CP) during guard interval is added to each symbol to prevent ISI and ICI. Discrete Fourier transform is performed on the guard interval removed symbol at the receiver. The received symbol is as follows

$$Y(n, k) = H(n, k)X(n, k) + W(n, k), \quad n = 0, \ldots, N_s - 1, \quad k = 0, \ldots, N_c - 1 \tag{1}$$

where $H(n, k)$ is complex channel coefficients for nth symbol and kth subcarrier, $X(n, k)$ is modulated input data, $W(n, k)$ is additive white Gaussian noise, N_c is the number of subcarriers per OFDM symbol, and N_s is the number of OFDM symbols per OFDM frame.

Then, the pilots are extracted, complete channel coefficients are estimated, and the binary information data is obtained.

In mobile communications, the transmitted signal arrives at the receiver through multiple paths due to reflections, scattering, and diffraction that causes delay, attenuation, and phase shift. This phenomenon is known as multipath channel. Another characteristic of the multipath channel is time variation that arises due to the movement of either transmitter or receiver. The time varying multipath channel can be characterised in frequency domain by B_c and in time domain by T_c.

The B_c can be obtained from a frequency correlation function (FCF) that describes the time varying channels' dispersion in frequency [13]. The FCF, $R(\Omega)$, for a wide sense stationary uncorrelated scattering (WSSUS) channel is given in (2),

$$R(\Omega) = \int_{-\infty}^{+\infty} P_h(\tau)\, e^{-j2\pi\Omega\tau}\, d\tau \tag{2}$$

where Ω is difference frequency variable, and $P_h(\tau)$ is power delay profile. B_c is defined as the bandwidth over which the normalised FCF function is above 0.5, 0.75, or 0.9 ($B_{c,0.5}$, $B_{c,0.75}$, $B_{c,0.9}$).

The T_c can be obtained from time correlation function (TCF) [13]. TCF, $R(\xi)$, for a WSSUS channel is given by

$$R(\xi) = \int_{-\infty}^{+\infty} S_h(f)\, e^{j2\pi\xi f}\, df \tag{3}$$

where ξ difference time variable and $S_h(f)$ is Doppler power spectrum. T_c is defined as the time over which the normalised TCF is above 0.5, 0.75, 0.9 ($T_{c,0.5}$, $T_{c,0.75}$, $T_{c,0.9}$).

3 MSE analytical formulation

In pilot aided channel estimation, selection of pilot pattern is important. The pilot symbols should be placed close enough to each other enable the system to follow the time and frequency variations of the channel, and far enough to increase the bandwidth efficiency. The lower bound for the pilot interval is determined according to the Nyquist sampling theorem in (4),

$$N_t \le \frac{1}{2 f_{d,\max} T_s}, \quad N_f \le \frac{1}{2\tau_{\max}\Delta f} \tag{4}$$

where N_t and N_f are spacing between pilot symbols in time and frequency direction respectively, T_s is OFDM symbol duration, Δf is subcarrier spacing, $f_{d,\max}$ is the maximum Doppler shift, and $\tau_{\max}$ is the maximum delay spread [14].

The estimation of the channel at the pilot frequencies can be based on least square (LS), and the LS estimate of channel at the pilot positions is given as

$$\hat{H}(n_p, k_p) = \frac{Y(n_p, k_p)}{X(n_p, k_p)} = H(n_p, k_p) + \frac{W(n_p, k_p)}{X(n_p, k_p)} = H(n_p, k_p) + N(n_p, k_p) \tag{5}$$

where $X(n_p, k_p)$ denotes the pilots, $N(n_p, k_p)$ denotes the noise term at pilot locations n_p in time direction and k_p in frequency direction.

Then, the final estimates of complete channel coefficients $[\tilde{H}(n, k)]$ are obtained from $\hat{H}(n_p, k_p)$ using appropriate interpolation techniques. Let $\tilde{H}(n, k)$ denote the final estimate of channel at nth symbol and kth subcarrier, and $E\{.\}$ denote the expected value; then, channel estimation MSE can be calculated as follows

$$\sigma_e^2 = E\left\{\left|\tilde{H}(n, k) - H(n, k)\right|^2\right\} \tag{6}$$

The N_f and N_t values that minimise the MSE of the CIR estimation must be determined. If there is no noise or interference, the CIR can perfectly be estimated by using an ideal interpolator as in (7),

$$H[n, k] = \sum_{i=-\infty}^{+\infty} \sum_{\ell=-\infty}^{+\infty} H_S[n + i, k + \ell]\omega_p[i, \ell] \tag{7}$$

where $H_S[n, k]$ is equal to $H[n, k]$ for the pilot symbol and zero otherwise, and $\omega_p[i, \ell]$ is the ideal 2D sinc filter coefficients.

The real LS estimates are noisy samples of the channel that are used as the input to the 2D non-ideal estimation filter to obtain the CIR estimate $\tilde{H}[n, k]$,

$$\tilde{H}[n, k] = \sum_{i=-\infty}^{+\infty} \sum_{\ell=-\infty}^{+\infty} \hat{H}_S[n + i, k + \ell]\, \omega[i, \ell] \tag{8}$$

where $\hat{H}_S[n, k]$ is equal to $\hat{H}[n, k]$ for the pilot symbol and zero otherwise, and $\omega[i, \ell]$ denotes the coefficient of the interpolator.

The estimation error is calculated as (see (9)) where $N_S[n, k]$ is equal to $N[n, k]$ for the pilot positions and zero otherwise, and $\omega_e(i, \ell)$denotes the error due to imperfect estimation filter.

Applying 2D discrete time Fourier transform (DTFT) to the (9), the error can be rewritten as follows

$$E(\omega_n, \omega_k) = H_S(\omega_n, \omega_k)W_e(\omega_n, \omega_k) + N_S(\omega_n, \omega_k)W(\omega_n, \omega_k) \tag{10}$$

Applying 2D discrete Parseval's theorem to (10), the channel

IET Commun., 2015, Vol. 9, Iss. 15, pp. 1915–1923
© The Institution of Engineering and Technology 2015

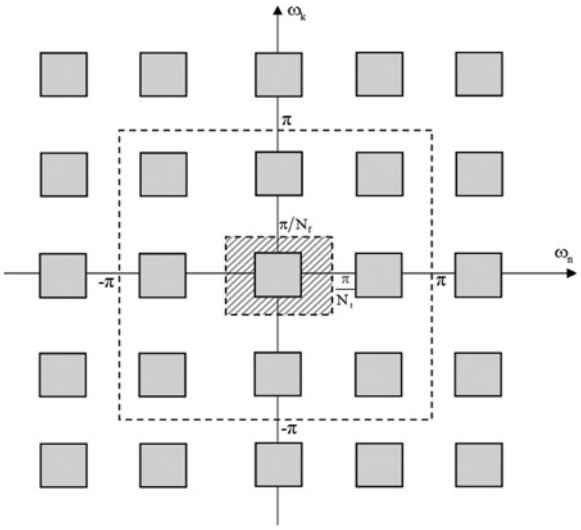

Fig. 1 *Channel's sampled power spectral density*

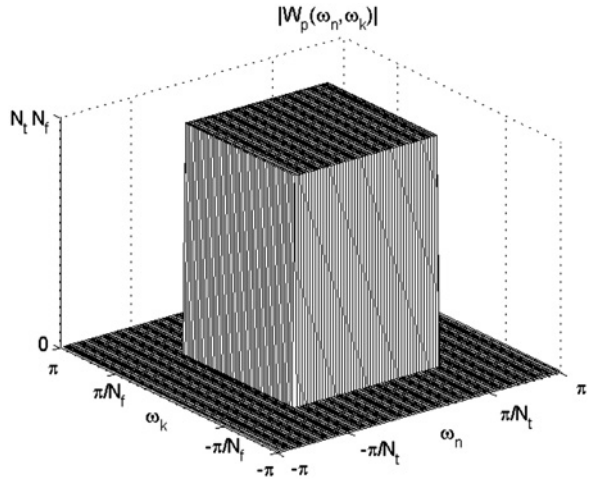

Fig. 2 *Ideal 2D sinc filter's magnitude response*

estimation MSE can be written as

$$\sigma_{\mathrm{e}}^2 = \frac{1}{4\pi^2}\int_{-\pi}^{\pi}\int_{-\pi}^{\pi} S_{H_{\mathrm{S}}}(\omega_n, \omega_k)\left|W_{\mathrm{e}}(\omega_n, \omega_k)\right|^2 \mathrm{d}\omega_k\, \mathrm{d}\omega_n + \frac{\sigma_n^2}{4\pi^2 N_{\mathrm{f}} N_{\mathrm{t}}}\int_{-\pi}^{\pi}\int_{-\pi}^{\pi}\left|W(\omega_n, \omega_k)\right|^2 \mathrm{d}\omega_k\, \mathrm{d}\omega_n \tag{11}$$

where $S_{H_{\mathrm{S}}}$ is the sampled channel's power spectral density as shown in Fig. 1 and σ_n^2 is the variance of the noise.

The 2D DTFT of the error filter is given by

$$W_{\mathrm{e}}(\omega_n, \omega_k) = W(\omega_n, \omega_k) - W_{\mathrm{p}}(\omega_n, \omega_k) \tag{12}$$

Because

$$W_{\mathrm{p}}(\omega_n, \omega_k) = \begin{cases} N_{\mathrm{f}}N_{\mathrm{t}}, & \left|\omega_k\right| \le \pi/N_{\mathrm{f}},\ \left|\omega_n\right| \le \pi/N_{\mathrm{t}} \\ 0, & \text{otherwise} \end{cases} \tag{13}$$

as shown in Fig. 2, the error can be rewritten as

$$W_{\mathrm{e}}(\omega_n, \omega_k) = \begin{cases} W(\omega_n, \omega_k) - N_{\mathrm{f}}N_{\mathrm{t}}, & \left|\omega_k\right| \le \pi/N_{\mathrm{f}},\ \left|\omega_n\right| \le \pi/N_{\mathrm{t}} \\ W(\omega_n, \omega_k), & \text{otherwise} \end{cases} \tag{14}$$

Because the interpolator filters most of the energy of the channel replicas inside the area $|\omega_k| \le \pi/N_{\mathrm{f}}$, $|\omega_n| \le \pi/N_{\mathrm{t}}$ as shown in Fig. 1, the error introduced by the first term of (11) in this area is negligible, and (11) can be approximated as

$$\sigma_{\mathrm{e}}^2 \simeq \frac{1}{4\pi^2}\int_{-\frac{\pi}{N_t}}^{\frac{\pi}{N_t}}\int_{-\frac{\pi}{N_f}}^{\frac{\pi}{N_f}} S_{H_{\mathrm{S}}}(\omega_n, \omega_k)\left|W(\omega_n, \omega_k) - N_{\mathrm{f}}N_{\mathrm{t}}\right|^2 \mathrm{d}\omega_k\, \mathrm{d}\omega_n + \frac{\sigma_n^2}{4\pi^2 N_f N_t}\int_{-\pi}^{\pi}\int_{-\pi}^{\pi}\left|W(\omega_n, \omega_k)\right|^2 \mathrm{d}\omega_k\, \mathrm{d}\omega_n \tag{15}$$

The optimum N_{f} and N_{t} can be determined by solving

$$\left.\frac{\partial\sigma_{\mathrm{e}}^2}{\partial N_{\mathrm{f}}}\right|_{N_{\mathrm{f}}=\hat{N}_{\mathrm{f}}} = 0 \quad \text{and} \quad \left.\frac{\partial\sigma_{\mathrm{e}}^2}{\partial N_{\mathrm{t}}}\right|_{N_{\mathrm{t}}=\hat{N}_{\mathrm{t}}} = 0 \tag{16}$$

Since the limits of the integral are independent from the partial derivative variables,

$$\frac{\partial}{\partial N_{\mathrm{t}}}\frac{\partial}{\partial N_{\mathrm{f}}}\left[\frac{\sigma_n^2}{4\pi^2}\int_{-\pi}^{\pi}\int_{-\pi}^{\pi}\left|W(\omega_k, \omega_n)\right|^2 \mathrm{d}\omega_k\, \mathrm{d}\omega_n\right] = 0 \tag{17}$$

The partial derivative of the first term of (15) with respect to N_{f} and N_{t} must be equal to zero for the optimum $\hat{N}_{\mathrm{f}}$ and $\hat{N}_{\mathrm{t}}$ values, as in (18): (see (18)). In the presence of noise, the term $W_e(\omega_n, \omega_k)$ in (18) always contains non-zero values, as given in (19), and its absolute value is greater than zero.

$$W_{\mathrm{e}}(\omega_n, \omega_k) = \begin{cases} 0, & W(\omega_n, \omega_k) \Leftrightarrow W_{\mathrm{p}}(\omega_n, \omega_k) \\ \text{non-zero values}, & \text{otherwise} \end{cases} \tag{19}$$

$$\begin{aligned} e[n, k] &= \tilde{H}[n, k] - H[n, k] \\ &= \sum_{i=-\infty}^{+\infty}\sum_{\ell=-\infty}^{+\infty}\hat{H}_{\mathrm{S}}[n+i, k+\ell]\,\omega[i, \ell] - \sum_{i=-\infty}^{+\infty}\sum_{\ell=-\infty}^{+\infty}H_{\mathrm{S}}[n+i, k+\ell]\,\omega_{\mathrm{p}}[i, \ell] \\ &= \sum_{i=-\infty}^{+\infty}\sum_{\ell=-\infty}^{+\infty}\left(H_{\mathrm{S}}[n+i, k+\ell] + N_{\mathrm{S}}[n+i, k+\ell]\right)\omega[i, \ell] - \sum_{i=-\infty}^{+\infty}\sum_{\ell=-\infty}^{+\infty}H_{\mathrm{S}}[n+i, k+\ell]\,\omega_{\mathrm{p}}[i, \ell] \\ &= \sum_{i=-\infty}^{+\infty}\sum_{\ell=-\infty}^{+\infty}H_{\mathrm{S}}[n+i, k+\ell]\underbrace{\left(\omega[i, \ell] - \omega_{\mathrm{p}}[i, \ell]\right)}_{\omega_{\mathrm{e}}[i,\ell]} + \sum_{i=-\infty}^{+\infty}\sum_{\ell=-\infty}^{+\infty}N_{\mathrm{S}}[n+i, k+\ell]\,\omega[i, \ell] \end{aligned} \tag{9}$$

© The Institution of Engineering and Technology 2015

Keeping that in mind, (18) can be equal to zero if and only if the condition in (20) is fulfilled.

$$\frac{\partial}{\partial N_t}\frac{\partial}{\partial N_f}\left[\int_{-\frac{\pi}{N_t}}^{\frac{\pi}{N_t}}\int_{-\frac{\pi}{N_f}}^{\frac{\pi}{N_f}} S_{H_s}(\omega_n, \omega_k)\,d\omega_k\,d\omega_n\right]\Bigg|_{\substack{N_t=\hat{N}_t\\N_f=\hat{N}_f}} = 0 \quad (20)$$

(see (21)).

After taking the partial derivative of (20) with respect to N_f, and using the symmetrical property of power spectral density, (21) can be rewritten as follows:

$$\frac{\partial}{\partial N_t}\left[\int_{-(\pi/N_t)}^{(\pi/N_t)}\left[\left(-\frac{2\pi}{N_f^2}\right)S_{H_s}\left(\omega_n, \frac{\pi}{N_f}\right)\right]d\omega_n\right]\Bigg|_{\substack{N_t=\hat{N}_t\\N_f=\hat{N}_f}} = 0 \quad (22)$$

Then, (22) can be reorganised as

$$\left(-\frac{2\pi}{N_f^2}\right)\left[S_{H_s}\left(\frac{\pi}{N_t}, \frac{\pi}{N_f}\right)\left(-\frac{\pi}{N_t^2}\right) - S_{H_s}\left(\frac{\pi}{N_t}, -\frac{\pi}{N_f}\right)\left(\frac{\pi}{N_t^2}\right)\right]\Bigg|_{\substack{N_t=\hat{N}_t\\N_f=\hat{N}_f}} = 0 \quad (23)$$

The channel estimation MSE can directly be expressed as a function of a channel's sampled power density as follows:

$$\left(\frac{4\pi^2}{N_f^2N_t^2}\right)\left[S_{H_s}\left(\frac{\pi}{N_t}, \frac{\pi}{N_f}\right)\right]\Bigg|_{\substack{N_t=\hat{N}_t\\N_f=\hat{N}_f}} = 0 \quad (24)$$

The $\hat{N}_f$ and $\hat{N}_t$ values that make the S_{H_S} value zero in (24) are determined as the optimum N_f and N_t.

4 Analysis and results

In this study, the impact of pilot density on channel estimation error performance is evaluated by analytical results. Pilot symbols are inserted as 2D rectangular. N_f and N_t values that yield the minimum S_{H_S} value in dB are determined as $\hat{N}_f$, $\hat{N}_t$. A propagation measurement based channel model was used in the calculations to adapt the system to real-time conditions. The propagation measurements were previously carried out in Manchester city centre within the middle 20 MHz section 2110–2170 MHz band using a CHIRP sounder. Details of the sounder and the measurements can be found in [15]. Five different frequency selective channels that represent mild, moderate, and strong multipath spreads are chosen, and these data are referred to as Channel 1 (Ch1), Channel 2 (Ch2), Channel 3 (Ch3), Channel 4 (Ch4), and Channel 5 (Ch5). The average impulse responses (IRs) for the channels are depicted in Fig. 3, while the system parameters and channel properties are given in Table 1. To create different time selective channels the simulator that uses the Clarke and Gans model is used [16]. The Rayleigh fading envelopes are obtained for 5, 92, 166, 222, 370 Hz Doppler frequencies and 2 GHz carrier frequency, and these fadings are applied to all paths.

4.1 Optimum pilot intervals

The impact of pilot density on channel power spectral density's envelope is evaluated for various N_f and N_t, then the N_f and N_t values that yield the minimum normalised S_{H_S} value are defined as the optimum pilot symbols ($\hat{N}_f$ and$\hat{N}_t$). The simulations are performed for all the N_f and N_t values which fulfil (4). However, the results between the intervals which contain the minimum value are shown in Fig. 4. Because Ch1 represents the lowest frequency selectivity, 5 and 370 Hz Doppler frequencies cause the lowest and the highest time selectivity; the results are given in the following figures for mentioned ones, while others are saved to be used during the curve-fitting process.

The changes in the envelope of normalised power spectral densities versus N_f and N_t, for Ch1, 5 and 370 Hz Doppler frequency are given Figs. 4*a* and *b*. In Fig. 4 the ($\hat{N}_f$, $\hat{N}_t$) values are shown with a circle.

Since Ch1's frequency selectivity and for 5 Hz Doppler frequency time selectivity is low, optimum pilot density is obtained at larger N_f and N_t values (Fig. 4*a*). With the increase of a channel's time selectivity, the optimum N_t value is decreased and optimum N_f value remains almost the same.

After determining the optimum pilot density, the optimum pilot symbol interval in frequency (Δf_{opt}) and time (Δt_{opt}) direction is calculated from $\hat{N}_f$, $\hat{N}_t$ as follows

$$\Delta f_{opt} = \hat{N}_f.\Delta f \quad (25)$$

$$\Delta t_{opt} = \hat{N}_t.T_s \quad (26)$$

4.2 Proposed adaptive pilot placement

The optimum pilot symbol intervals are obtained through (25) and (26) for five different frequency selective channels and Doppler frequencies. In this study, unlike the previous studies, relating these optimum intervals to a channel's coherence time and bandwidth is the aim. To achieve this goal, coherence time and bandwidth with 0.5, 0.75, and 0.9 correlation coefficients, which are frequently used in the literature, are related to the optimum intervals by using the following equations.

$$F_{f,\psi}(\varphi) = \frac{B_{c,\psi}(\varphi)}{\Delta f_{opt}(\varphi)} \quad \begin{matrix}\varphi = 1, 2, \ldots, 5\\ \psi = 0.5,\ 0.75,\ 0.9\end{matrix} \quad (27)$$

$$F_{t,\psi}(\gamma) = \frac{T_{c,\psi}(\gamma)}{\Delta t_{opt}(\gamma)} \quad \begin{matrix}\gamma = 1, 2, \ldots, 5\\ \psi = 0.5,\ 0.75,\ 0.9\end{matrix} \quad (28)$$

Therein, φ is the number of channels, γ is the number of different Doppler frequencies, ψ is correlation coefficients, and $F_{f,\psi}$ and $F_{t,\psi}$ are the ratio parameters for frequency and time direction respectively. The statistical evaluation between the optimum pilot symbol interval and channels' coherence bandwidth and coherence time is assessed for all cases, as well as the cumulative distribution functions (CDF) which are used for determining the probability of being lower or higher than a certain value or between two values in analysis. Thus, use of the generalised distribution functions gives rise to determining which correlation coefficient relates the parameters the best. Generalised CDF for the generalised ratio

$$\frac{\partial}{\partial N_t}\frac{\partial}{\partial N_f}\left[\frac{1}{4\pi^2}\int_{-\frac{\pi}{N_t}}^{\frac{\pi}{N_t}}\int_{-\frac{\pi}{N_f}}^{\frac{\pi}{N_f}} S_{H_s}(\omega_n, \omega_k)\underbrace{\left|W(\omega_n, \omega_k) - N_fN_t\right|^2}_{W_e(\omega_n,\omega_k)}d\omega_k d\omega_n\right]\Bigg|_{\substack{N_t=\hat{N}_t\\N_f=\hat{N}_f}} = 0 \quad (18)$$

$$\frac{\partial}{\partial N_t}\left[\int_{-(\pi/N_t)}^{(\pi/N_t)}\left[S_{H_s}\left(\omega_n, \frac{\pi}{N_f}\right)\left(-\frac{\pi}{N_f^2}\right) - S_{H_s}\left(\omega_n, -\frac{\pi}{N_f}\right)\left(\frac{\pi}{N_f^2}\right)\right]d\omega_n\right]\Bigg|_{\substack{N_t=\hat{N}_t\\N_f=\hat{N}_f}} = 0 \quad (21)$$

IET Commun., 2015, Vol. 9, Iss. 15, pp. 1915–1923
© The Institution of Engineering and Technology 2015

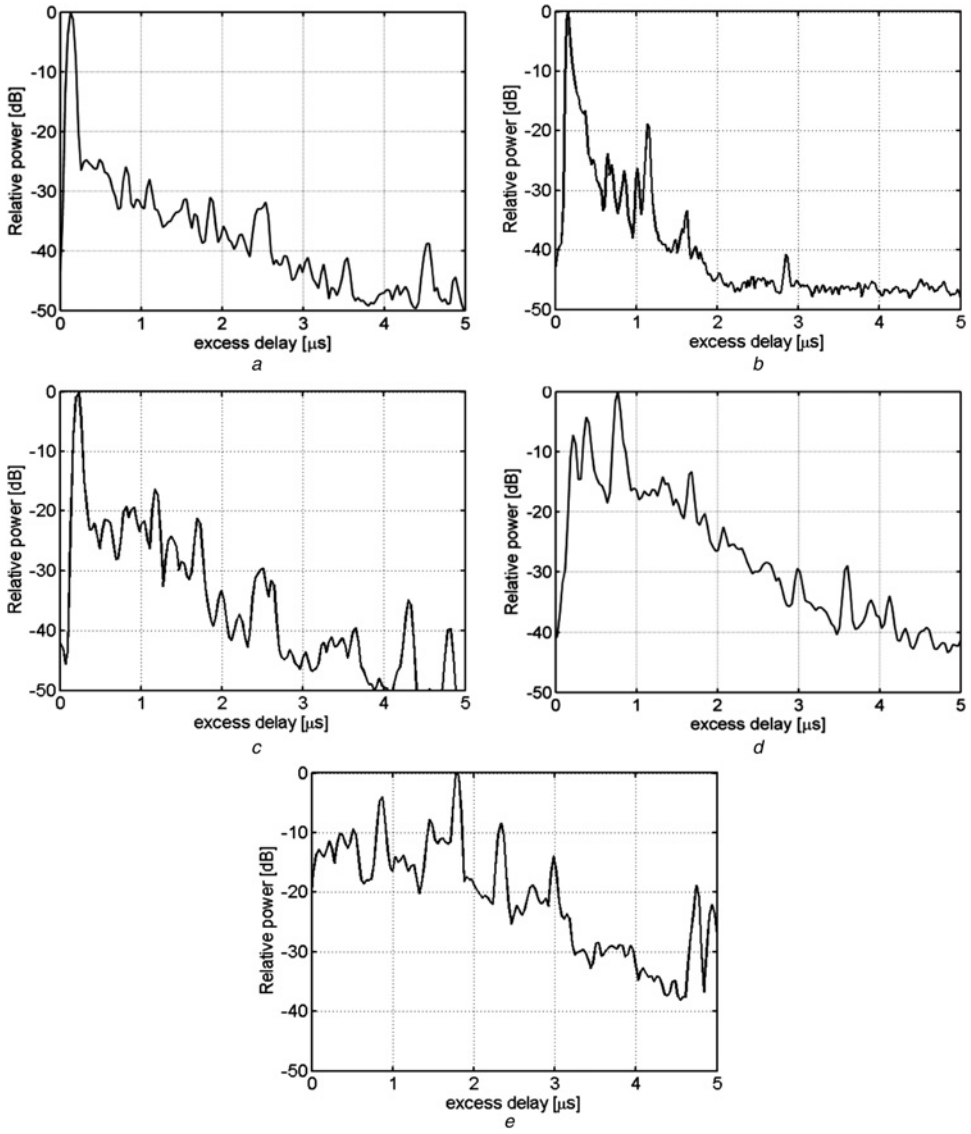

Fig. 3 *Average IRs for*

a Ch1
b Ch2
c Ch3
d Ch4
e Ch5

parameters ($\hat{F}_{\mathrm{f},\psi}$ and $\hat{F}_{\mathrm{t},\psi}$) are illustrated in Figs. 5*a* and *b* for B_{c}, and T_{c}, respectively. As seen in Fig. 5*a*, $\hat{F}_{\mathrm{f},\psi}$ is approximately 1.5 for 15% of all data at three correlation levels. As the $\hat{F}_{\mathrm{f},\psi}$ increases twofold, 20, 25, and 95% of data can be represented by 0.5, 0.75, and 0.9 correlation levels, respectively. 100% of data is covered at 3.8 $\hat{F}_{\mathrm{f},\psi}$ for 0.9 correlation. Similarly, for coherence times, 15% of data can be represented at all correlation levels by choosing the $\hat{F}_{\mathrm{t},\psi}$ as 0.8. When the $\hat{F}_{\mathrm{t},\psi}$ is about 1.6, the optimum pilot symbol interval in the time direction can be determined for 24, 34, and 85% of data at the corresponding correlation level. Complete data representation is obtained for the $\hat{F}_{\mathrm{t},\psi}$ of 2.6 for 0.9 correlation. Considering both the data representation percentage and margin of error for the fixed 95% confidence interval, the optimum pilot symbol intervals can be expressed best with coherence bandwidth and time at 0.9 correlation. It is also seen from the figures that the $\hat{F}_{\mathrm{f},0.9}$ varies between 1.28–3.80, and for $\hat{F}_{\mathrm{t},0.9}$ between 0.71–2.60. The estimated optimum pilot symbol intervals $\Delta\hat{f}_{\mathrm{opt}}$ and $\Delta\hat{t}_{\mathrm{opt}}$ can be calculated as follows

$$\Delta\hat{f}_{\mathrm{opt}}(\varphi) = \frac{B_{\mathrm{c},0.9}(\varphi)}{\hat{F}_{\mathrm{f},0.9}(\varphi)} \tag{29}$$

$$\Delta\hat{t}_{\mathrm{opt}}(\gamma) = \frac{T_{\mathrm{c},0.9}(\gamma)}{\hat{F}_{\mathrm{t},0.9}(\gamma)} \tag{30}$$

Then, the normalised root mean squared errors (NRMSE) between the estimated and actual optimum pilot symbol intervals are

Table 1 System parameters and channel properties

Number of users	One				
uplink/downlink	Downlink				
number of subcarriers (N_{c})	1024				
number of OFDM symbols (N_{s})	2048				
CP length	256				
transmission bandwidth	20 MHz				
channel model	Ch1	Ch2	Ch3	Ch4	Ch5
RMS delay spread, τ_{rms}, μs	0.078	0.217	0.249	0.364	0.767
fading type	Rayleigh				
doppler frequencies, Hz	5, 92, 166, 222, 370				

© The Institution of Engineering and Technology 2015

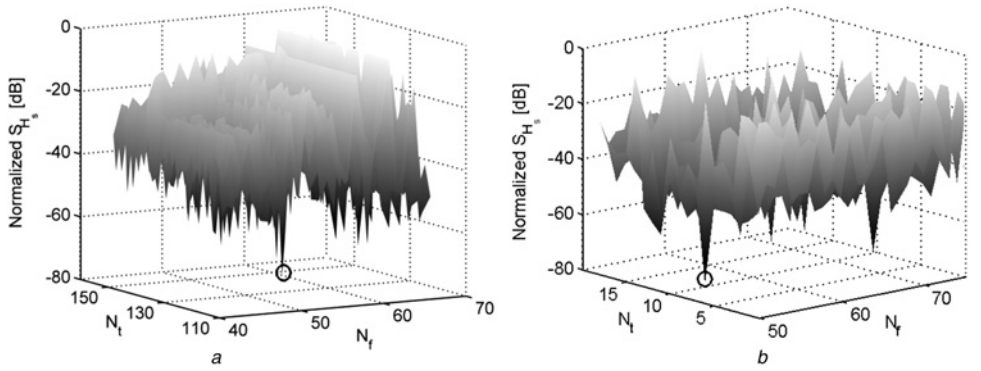

Fig. 4 *Changes in S_{H_S} values for Ch1 for*
a 5 Hz
b 370 Hz

calculated as in (31) and (32) and shown in Fig. 6.

$$\mathrm{NRMSE_f} = \frac{\sqrt{\frac{1}{5}\sum_{\varphi=1}^{5}\left[\Delta f_{\mathrm{opt}}(\varphi) - \Delta\hat{f}_{\mathrm{opt}}(\varphi)\right]^2}}{\max\left(\Delta f_{\mathrm{opt}}\right) - \min\left(\Delta f_{\mathrm{opt}}\right)} \tag{31}$$

$$\mathrm{NRMSE_t} = \frac{\sqrt{\frac{1}{5}\sum_{\gamma=1}^{5}\left[\Delta t_{\mathrm{opt}}(\gamma) - \Delta\hat{t}_{\mathrm{opt}}(\gamma)\right]^2}}{\max\left(\Delta t_{\mathrm{opt}}\right) - \min\left(\Delta t_{\mathrm{opt}}\right)} \tag{32}$$

By using these equations, $\hat{F}_{\mathrm{f},0.9}$ and $\hat{F}_{\mathrm{t},0.9}$ are calculated as 2.59 and 1.77, while NRMSEs are 0.115 and 0.107, respectively.To find the mathematical method that yields even lower NRMSE between the optimum pilot symbol interval and channels' coherence bandwidth and coherence time, widely used curve fitting methods are applied to data, and the goodness of the fits are compared in terms of NRMSE. Taking into account both simplicity and accuracy, the three fitting methods that yield the better performance among others (such as exponential, Gaussian, rational i.e.) are used, and the results are given in Figs. 7*a* and *b* for $B_{\mathrm{c},0.9}$, $T_{\mathrm{c},0.9}$, respectively. In figures, dashed lines refer to the linear polynomial, and dotted lines represent the power function, while a solid line shows the quadratic polynomial. The NRMSEs of the methods are 0.093, 0.029, and 0.016 for $B_{\mathrm{c},0.9}$ and 0.065, 0.033, and 0.014 for $T_{\mathrm{c},0.9}$, respectively.It is seen from the results that using a quadratic polynomial yields the minimum NRMSE. The mathematical relationships between $\Delta\hat{f}_{opt}$and $B_{\mathrm{c},0.9}$, $\Delta\hat{t}_{\mathrm{opt}}$and $T_{\mathrm{c},0.9}$ can be defined as follows

$$\Delta\hat{f}_{\mathrm{opt}} = -0.1142\left(B_{\mathrm{c},0.9}\right)^2 + 0.6836B_{\mathrm{c},0.9} - 0.0074 \tag{33}$$

$$\Delta\hat{t}_{\mathrm{opt}} = -0.05281\left(T_{\mathrm{c},0.9}\right)^2 + 1.13T_{\mathrm{c},0.9} - 0.03257 \tag{34}$$

The optimum pilot symbol interval in time and frequency direction can be expressed with one variable channel parameter as in (33) and (34) for time variant frequency selective channels. With the use of these proposed equations, the optimum pilot arrangement can be determined easily without high computational complexity, as in (24).

These equations, which are obtained from five characteristically different channel profiles, give similar results for other possible channel conditions. To test the accuracy of the proposed method, the optimum intervals are obtained for ITU test channels, using (24) and the proposed method, and results are given in Table 2 as an example. It is seen from the table that the theoretical values can be determined easily with the use of the proposed method with, on average, 90% accuracy.

To achieve higher bandwidth efficiency compared with fixed pilot placement that is commonly used in literature, an adaptive pilot pattern using the proposed method can be constructed. An example of such a pilot placement is shown in Figs. 8*a* and *b*. It is seen from the figures, In the case of user movement and changing channel conditions with time (multipath profile, Doppler frequency, etc.), there is no change in the pilot positions for the fixed placement. However, in adaptively placed pilot symbols, pilot positions are updated correspondingly. It is also seen from Fig. 8*b* that for the case of lower selectivity, fewer pilot symbols

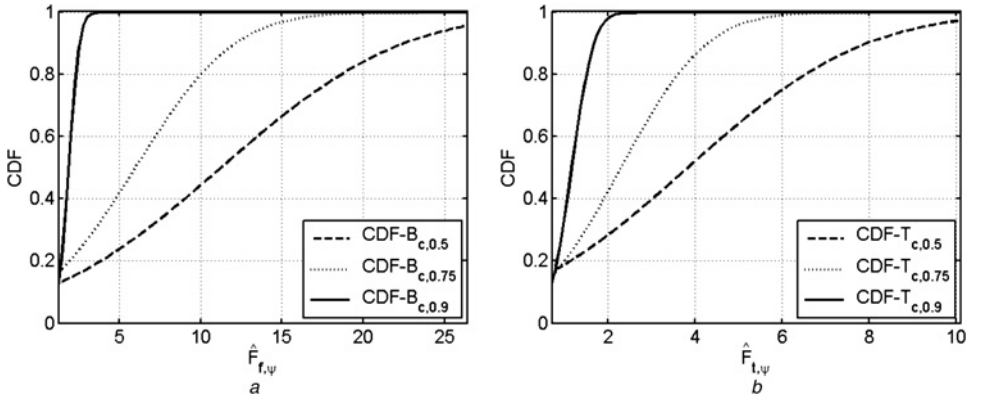

Fig. 5 *Generalized CDF for*
a B_c,
b T_c

IET Commun., 2015, Vol. 9, Iss. 15, pp. 1915–1923
© The Institution of Engineering and Technology 2015

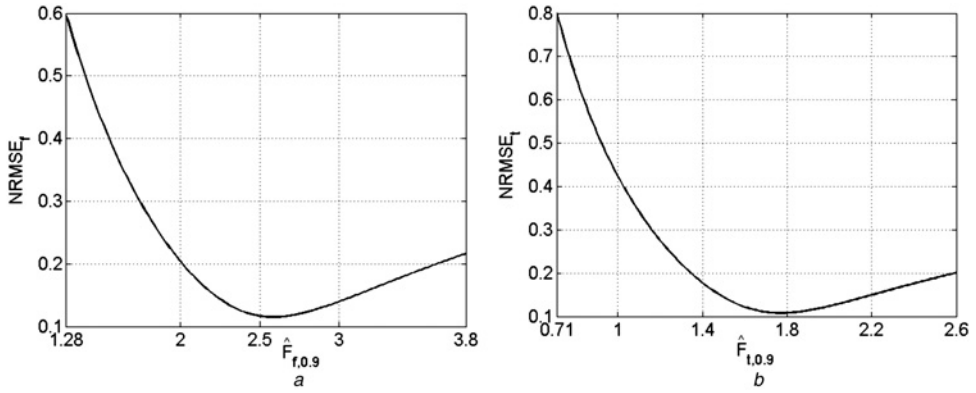

Fig. 6 *NRMSE versus*

a $\hat{F}_{f,0.9}$
b $\hat{F}_{t,0.9}$

can be used to estimate the channel, and vice versa for higher selectivity.

The block diagram of such a system is illustrated in Fig. 9. To use this adaptive pattern, the receiver must send the $B_{c,0.9}$, $T_{c,0.9}$ values to the transmitter via a feedback channel over a short period of time when the channel has stationary fading statistics. Then, the transmitter (adaptive pilot insertion block) determines the optimum

Table 2 Performance assessment of equations

Channel	Doppler, Hz	Δf_{opt}, MHz	Δt_{opt}, ms	$\Delta \hat{f}_{opt}$ (33), MHz	$\Delta \hat{t}_{opt}$ (34), ms
pedestrian-A	5	916	6.2	869	5.5
vehicular-A	70	97.5	4.3	109	4.8

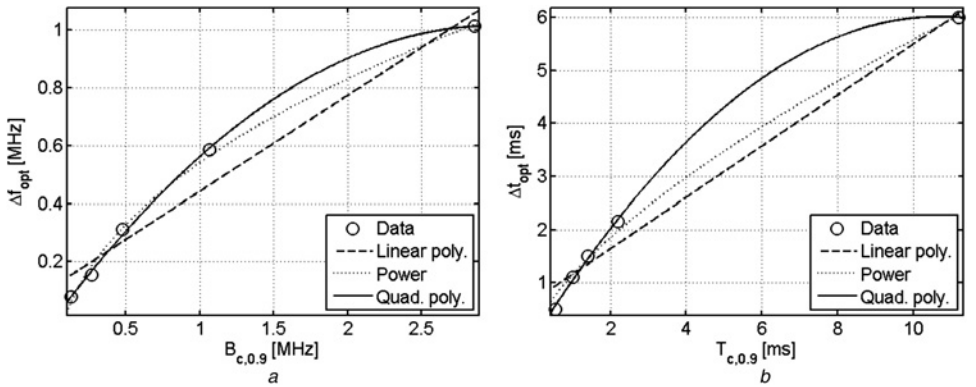

Fig. 7 *Curve fitting performances for*

a Δf_{opt}
b Δt_{opt}

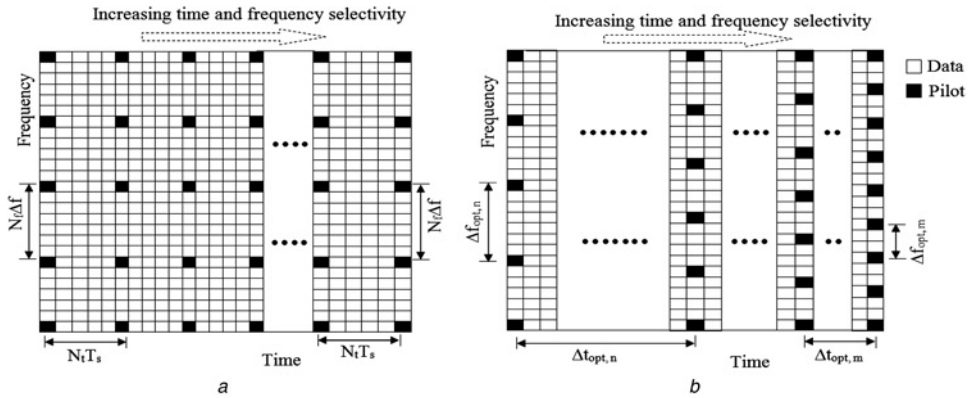

Fig. 8 *Example for*

a fixed
b adaptive placement of pilot symbols

© The Institution of Engineering and Technology 2015

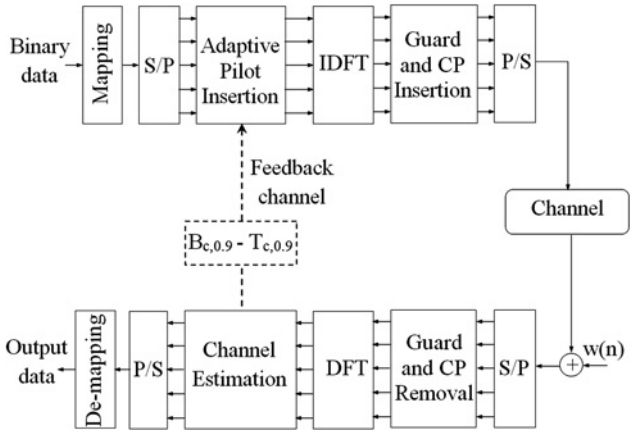

Fig. 9 *Structure of the proposed OFDM system with adaptive pilot placement*

pilot symbol interval using the proposed method [(33), (34)]. The details of the proposed adaptive system are explained in the flow chart in Fig. 10. In the first system, the initial values of B_c and T_c are assigned. Then, the OFDM symbol is sent via wireless radio channel. After that, the B_c and T_c values that are sent via the feedback channel are compared with the previous values in the adaptive pilot insertion block. If there is a change in B_c and T_c, time and/or frequency direction pilot pattern is modified accordingly; otherwise, no pilot symbols are inserted into the data. Therefore, a more efficient adaptive pilot pattern can be obtained. Using this adaptive pattern leads to minimising channel estimation error and maximising bandwidth efficiency for slow or fast changing channels.

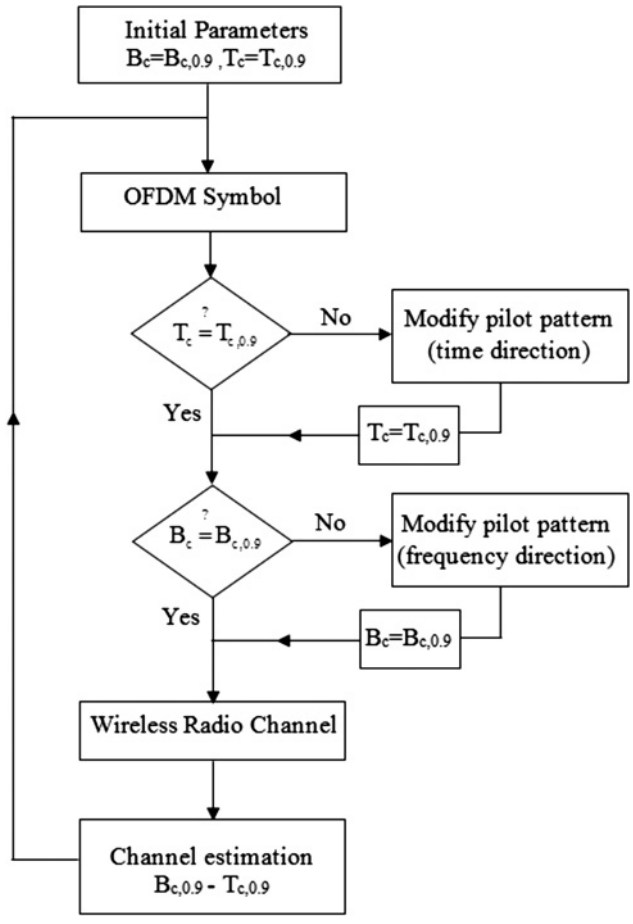

Fig. 10 *Flow chart of the proposed algorithm*

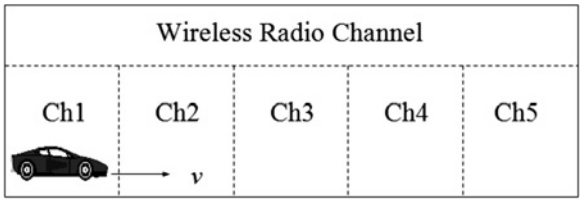

Fig. 11 *Channel change for the simulation*

4.3 Performance of proposed algorithm

In the end of the study, performance comparison of fixed pilot placement (Fig. 8*a*) and proposed adaptive pilot placement (Fig. 8*b*) is done. To do so, an OFDM system simulator is created with the parameters in Table 1. It is assumed in simulations that the vehicle passes through Ch1–Ch5, respectively, at the velocity of 50 km/h, as shown in Fig. 11, and stays in each channel for a second.

Performance comparison between fixed (rectangular pattern) and adaptive placement is assessed in terms of BER and shown in Fig. 12. In simulations, for the fixed placement, pilot spacing in frequency and time direction ($N_f \times N_t$) are chosen as 4×4, 8×8, and 16×16, while, for the proposed placement, as 50×45, 30×45, 15×45, 9×45, 4×45 which are calculated through (33) and (34) for each channel respectively. As seen from the figure, the use of the proposed adaptive placement provides notable BER performance improvement over the use of other ones. It can also be seen that the use of the adaptive placement closely follows the results for 4×4.

In spite of having good BER performance, using 4×4 fixed pilot placement causes considerable degradation in bandwidth efficiency compared with the proposed method. The bandwidth efficiency (η) can be obtained by the equation as follows

$$\eta = \frac{N_{UD}}{N_{UD} + N_P} \tag{35}$$

where N_P is number of pilot symbols, and N_{UD} is number of useful data in an OFDM frame, these can be calculated as follows

$$N_P = \frac{N_s}{N_t} \cdot \frac{N_c}{N_f} \tag{36}$$

$$N_{UD} = N_s.N_c - N_P \tag{37}$$

The bandwidth efficiencies are calculated for all of the pilot placements within each channel. Then mean of the results are given in Table 3. By using the adaptive placement, 99.7% bandwidth efficiency is achieved, that is, 6% higher than for 4×4.

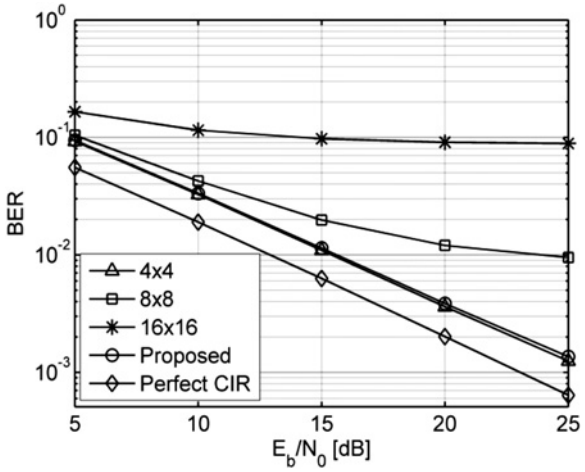

Fig. 12 *Performance comparison of the methods*

© The Institution of Engineering and Technology 2015

Table 3 Bandwidth efficiencies for different pilot placements

Pilot placement ($N_f \times N_t$)	Channel					Bandwidth efficiency, η
	Ch1	Ch2	Ch3	Ch4	Ch5	
proposed	50×45	30×45	15×45	9×45	4×45	0.997
fixed			4×4			0.937
			8×8			0.984
			16×16			0.996

5 Conclusions

In this study, channel estimation quality is assessed for different pilot densities, and types of fading analytically. Then a novel adaptively changed pilot placement based on channel parameters is proposed. To determine this placement, the pilot intervals that yield the minimum sampled channel's power spectral density value in frequency and time direction are determined and related to $B_{c,0.9}$ and $T_{c,0.9}$, respectively. The results demonstrate that using a quadratic polynomial yields the minimum normalised root MSE for fitted curve. Using this proposed method gives rise to constructing the adaptively placed pilot symbols according to changing channel conditions easily with reduced computational complexity while minimising channel estimation error and maximising bandwidth efficiency.

6 References

1 Bhatt, R., Shah, S.: 'Impact of sampling theorem on pilot aided channel estimation for OFDM based multi-carrier system'. Int. Conf. on Advances in Electronics and Electrical Engineering (AEEE), 2012, pp. 16–20

2 Coleri, M., Ergen, Puri A., Bahai, B.: 'Channel estimation techniques based on pilot arrangement in OFDM systems', *IEEE Trans. Broadcast.*, 2002, **48**, (3), pp. 223–229

3 Choi, J.W., Lee, Y.H.: 'Optimum pilot pattern for channel estimation in OFDM systems', *IEEE Trans. Wirel. Commun.*, 2005, **4**, (5), pp. 2083–2088

4 Abdelkader, Y.M., Jamal, E.A.: 'Optimal spacing design for pilots in OFDM systems over multipath fading channels', *Commun. Netw.*, 2010, **2**, (4), pp. 221–229

5 He, X., Song, R., Zhu, W.P.: 'Optimal pilot pattern design for compressed sensing-based sparse channel estimation in OFDM systems', *Circuits Syst. Signal Process.*, 2012, **31**, pp. 1379–1395

6 Imani, M., Bakhshi, H.: 'The tight bound for the number of pilots in channel estimation for OFDM systems', *Commun. Netw.*, 2012, **4**, (2), pp. 146–150

7 Asadi, A., Tazehkand, B.M.: 'New method to channel estimation in OFDM systems based on wavelet transform', *Int. J. Digit. Inf. Wirel. Commun.*, 2013, **3**, (1), pp. 1–9

8 Youssefi, M.A., Eiabbadi, J.: 'Pilot design optimization using modified differential evolution algorithm in SISO and MIMO OFDM systems', *J. Basic Appl. Sci. Res.*, 2010, **2**, (6), pp. 6260–6267

9 Fertl, P., Matz, G.: 'Channel estimation in wireless OFDM systems with irregular pilot distribution', *IEEE Trans. Signal Process.*, 2010, **58**, (6), pp. 3180–3194

10 Ribeiro, C.M.N.G.: 'Channel and frequency offset estimation schemes for multicarrier systems'. PhD dissertation, The University of Aveiro, Department of Electronics, Telecommunications and Informatics, Portugal, 2010

11 Simko, M., Diniz, P.S.R., Wang, Q., *et al.*: 'New insights in optimal pilot symbol patterns for OFDM Systems'. Wireless Communications and Networking Conf. (WCNC), China, 2013

12 Engiz, B.K., Kurnaz, C., Sezgin, H.: 'Performance analysis of pilot arrangement for OFDM systems over time varying frequency selective channels'. The Eighth IEEE Int. Conf. on Wireless and Mobile Computing, Networking and Communications (WiMob), 2012, pp. 113–117

13 Parsons, J.D.: 'The mobile radio propagation' (John Wiley & Sons Ltd, England, 1992)

14 Hoeher, P., Kaiser, S., Robertson, P.: 'Two-dimensional pilot-symbol-aided channel estimation by wiener filtering', *IEEE Int. Conf. Acoust. Speech Signal Process.*, 1997, **3**, pp. 1845–1848

15 Salous, S., Gokalp, H.: 'Medium and large scale characterization of UMTS allocated frequency division duplex channels', *IEEE Trans. Veh. Technol.*, 2007, **56**, (5), pp. 2831–2843

16 Cho, Y.S., Kim, J., Yang, W., *et al.*: 'MIMO-OFDM wireless communications with MATLAB' (John Wiley& Sons Ltd., 2010)

© The Institution of Engineering and Technology 2015

Copyright of IET Communications is the property of Institution of Engineering & Technology and its content may not be copied or emailed to multiple sites or posted to a listserv without the copyright holder's express written permission. However, users may print, download, or email articles for individual use.